Neuron, Volume *107*

Supplemental Information

Short-Term Plasticity at Hippocampal Mossy Fiber Synapses Is Induced by Natural Activity Patterns and Associated with Vesicle Pool Engram Formation

David Vandael, Carolina Borges-Merjane, Xiaomin Zhang, and Peter Jonas

Figure S1, related to Figure 2. A highly sensitive induction mechanism of hippocampal mossy fiber PTP at near-physiological temperature

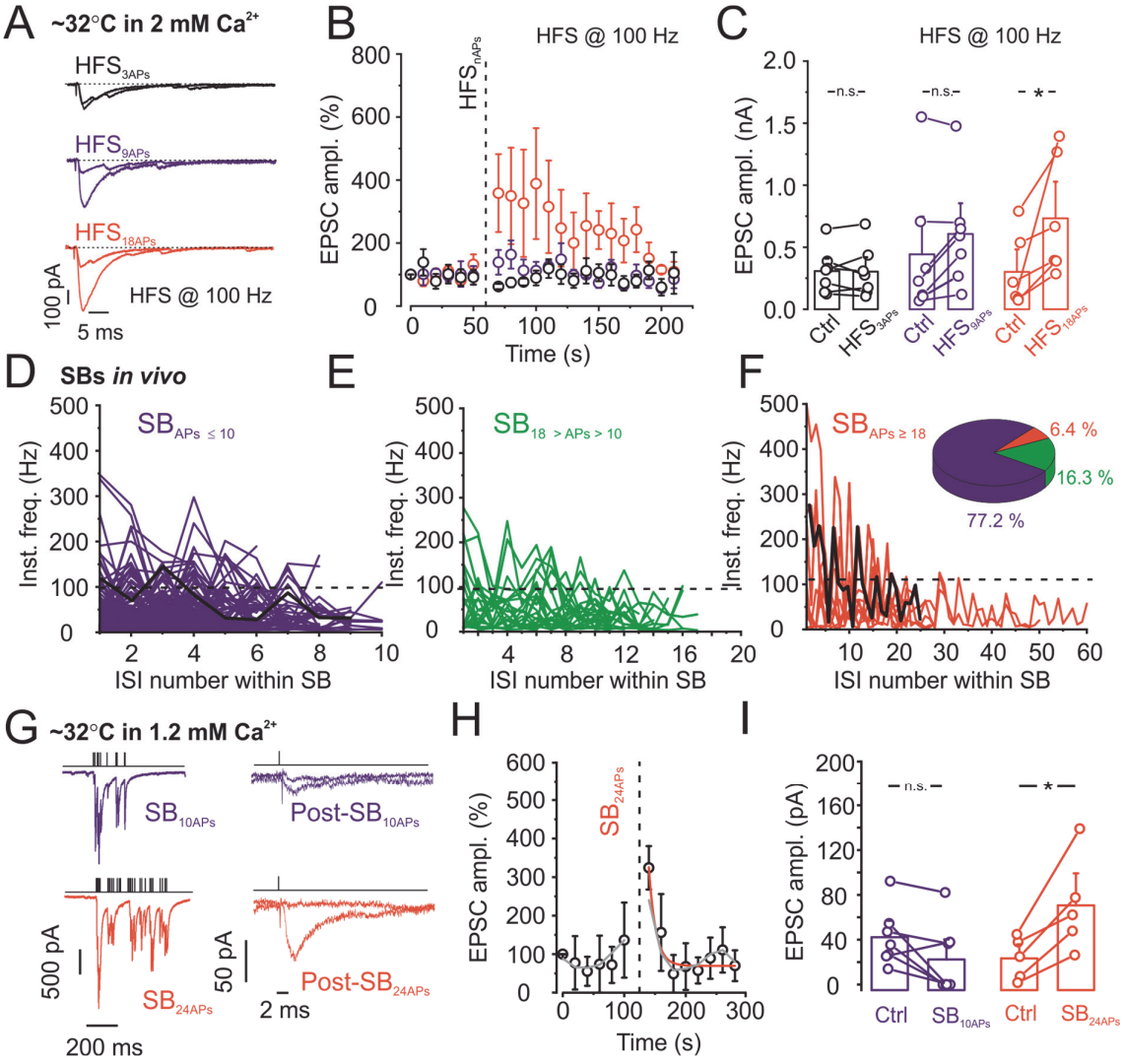

(**A**) Mossy fiber EPSCs under control conditions (black traces) and after HFS_{3APs} (black), HFS_{9APs} (blue), and HFS_{18APs} (red) at near-physiological temperature.
(**B**) Plot of average EPSC peak amplitude against experimental time. HFS_{3APs} (black), HFS_{9APs} (blue), and HFS_{18APs} (red) were applied at the time points indicated by the vertical dashed line.
(**C**) Summary bar graph of PTP at near-physiological temperature. Boxes indicate mean values, error bars denote SEM, and circles show data from individual experiments. In total, data were obtained from 9 mossy fiber terminal–CA3 pyramidal neuron recordings. *, $p < 0.05$.
(**D–F**) Plot of instantaneous frequency against ISI number for SBs with ≤ 10 APs (D), 11 – 17 APs (E), and ≥ 18 APs (F). Black line in (D) and (E) indicates the SB chosen for subsequent paired recording experiments. Black horizontal dashed line represents 100 Hz frequency used in standard PTP induction protocols.

(**G**) SBs induce PTP at near-physiological temperature and 1.2 mM extracellular Ca^{2+} concentration. Left, EPSCs evoked by SB_{10APs} and SB_{24APs}. Right, EPSCs under control conditions and after PTP induction.
(**H**) Plot of average EPSC peak amplitude against experimental time. SB_{24APs} was applied at the time point indicated by the vertical dashed line.
(**I**) Summary bar graph of PTP at near-physiological temperature and 1.2 mM extracellular Ca^{2+} concentration. As EPSC peak amplitudes in 1.2 mM Ca^{2+} were small, the second EPSC in a 50-Hz train was used for analysis in (H) and (I). Data from 9 pairs. *, $p < 0.05$.

Figure S2, related to Figure 3. Comparison of RRP size estimates for different fitting ranges

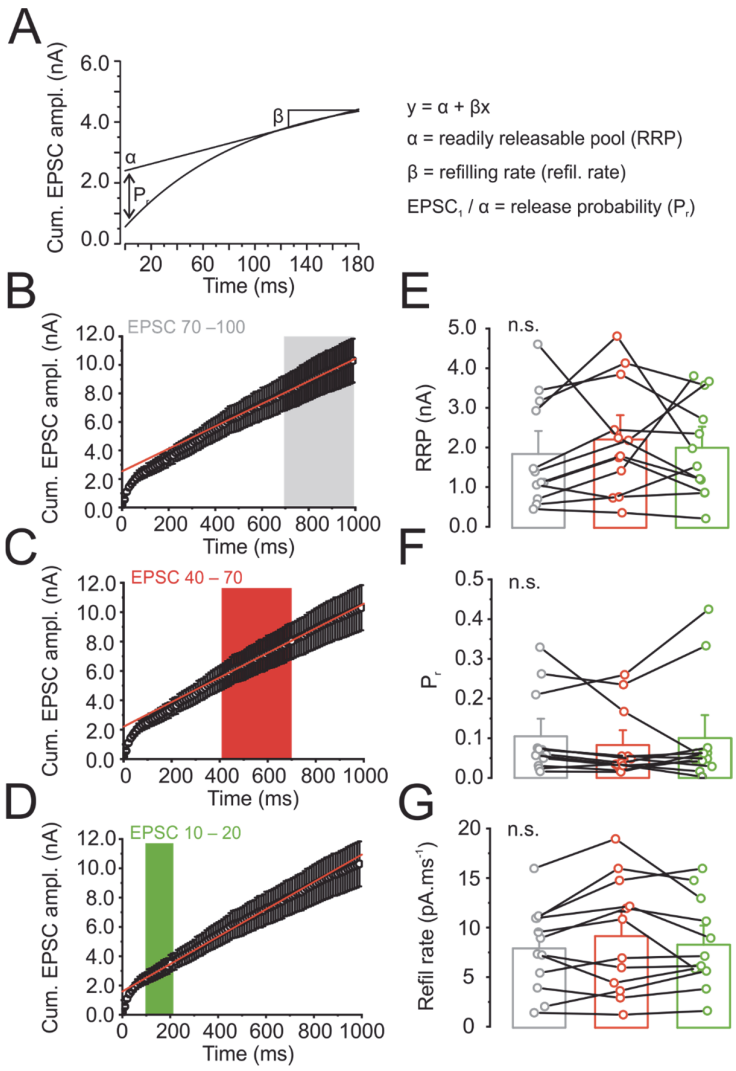

(**A**) Schematic illustration of pool analysis using the SMN method (Schneggenburger et al., 1999; Neher, 2015). Cumulative EPSC peak amplitude during a train stimulation was plotted against time, and data were analyzed by linear regression of the last 3–5 data points. The size of the RRP was determined as the intersection of the regression line with the ordinate, P_r was measured as the ratio of the first EPSC amplitude over RRP size, and refilling rate was obtained from the slope of the regression line.
(**B–D**) Analysis of cumulative EPSC data (100 stimuli, 100 Hz in presynaptic cell-attached stimulation) using the SMN method (Schneggenburger et al., 1999) for different fitting ranges (points 70–100 in (B), gray box; 40–70 in (C), red box; 10–20 in (D), green box).
(**E–G**) Comparison of RRP (E), P_r (F), and refilling rate (G) for the three different fitting ranges. Parameter estimates for the different fitting ranges were similar.

Figure S3, related to Figure 3. Analysis of RRP size in the presence of a low-affinity competitive antagonist reducing AMPA receptor saturation and desensitization

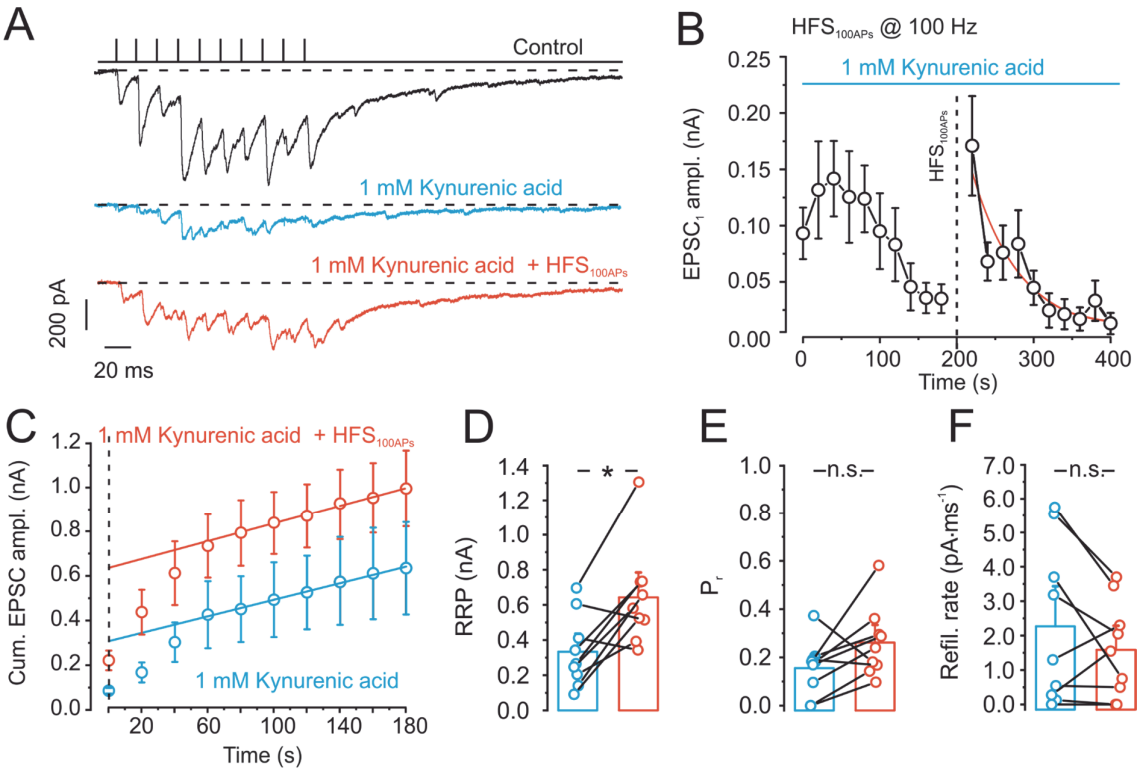

(**A**) Plot of EPSC traces under control conditions (black), in the presence of 1 mM of the low-affinity competitive AMPA receptor antagonist kynurenic acid (light blue), and 20 s after subsequent application of HFS_{100APs} (red).

(**B**) Plot of EPSC peak amplitude against experimental time during application of 1 mM kynurenic acid (horizontal blue continuous line) and subsequent application of HFS_{100APs} (vertical black dashed line). The red curve represents an exponential function fit to the PTP decay phase.

(**C**) Plot of cumulative EPSC peak amplitude during a train stimulation against time. Light blue, control data; red, data 20 s after HFS_{100APs}. Data points during the last 3–5 stimuli (at time points ≥ 100–140 ms) were fit by linear regression.

(**D–F**) Summary bar graphs of RRP (D), P_r (E), and refilling rate (F). PTP primarily increased the RRP size, but was associated with much smaller changes in P_r and refilling rate, similar to the results in the absence of the low-affinity competitive AMPA receptor antagonist (**Figures 3**D–3H).

Figure S4, related to Figure 3. Analysis of RRP size using models with time-dependent refilling rate or multiple pools

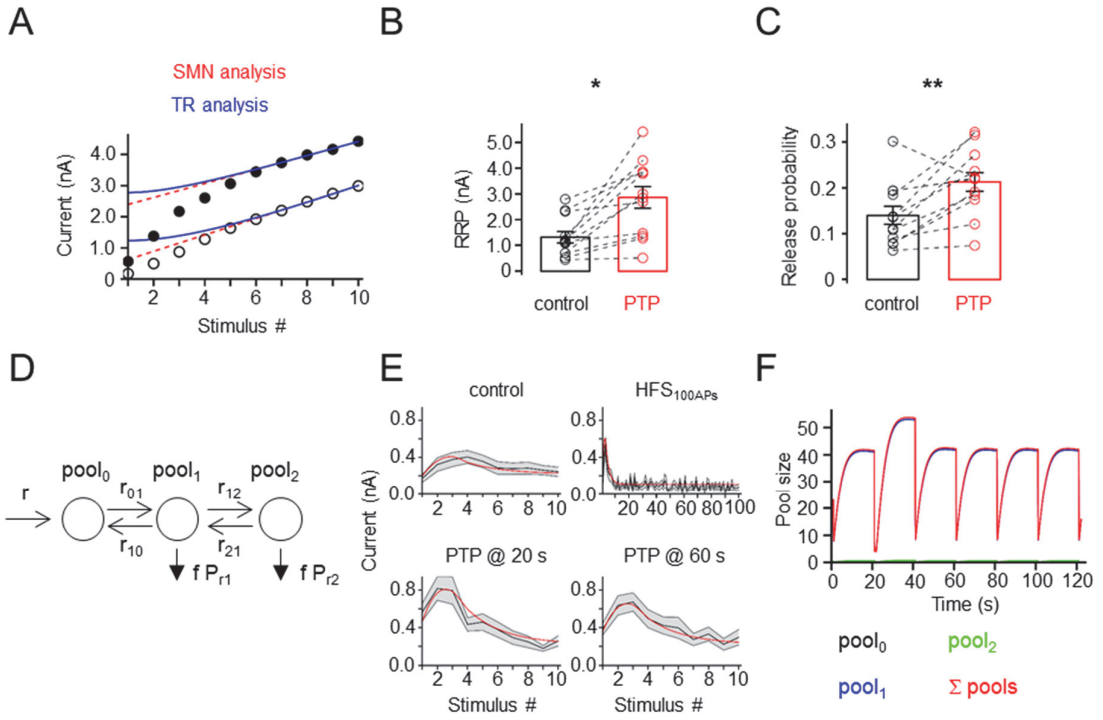

(**A**) Analysis of cumulative EPSC data before and after HFS_{100APs}. Open circles, control data; filled circles, data after HFS_{100APs}. Blue curve indicates fit according to the TR method (Thanawala and Regehr, 2013), assuming that refilling rate increases as release sites are vacated. Red dashed line shows fit according to the SMN method (Schneggenburger et al. 1999), assuming that refilling rate is constant.
(**B** and **C**) Summary bar graphs of RRP size (B) and P_r (C) estimated according to the TR model. Note that the size of the RRP is consistently larger with the TR model than with the SMN model. *, $p < 0.05$; **, $p < 0.01$. Data from 12 pairs.
(**D**) Structure of the three-pool model. The three pools in the model were intended to represent docked, primed, and superprimed vesicle pool (Lee et al., 2013; Taschenberger et al., 2016). f indicates facilitation factor, P_{r1} and P_{r2} indicate different release probabilities of primed and superprimed vesicles, respectively. For additional details, see STAR Methods and Table S2.
(**E**) Analysis of experimental stimulus train responses with the 3-pool model. Top left, control; top right, HFS_{100APs}; bottom left, PTP 20 s after HFS; bottom right, PTP 60 s after HFS. Black line, mean from 12 pairs; gray lines and shaded area, ± SEM range; red line, model prediction.
(**F**) Plot of size of the three pools as a function of time. Black, $pool_0$; blue, $pool_1$; green, $pool_2$; red, sum of all pools. Test stimulations (10 APs at 50 Hz) were applied every 20 s; HFS_{100APs} was simulated at 20 s (dashed vertical line). Note that $pool_2$ was only minimally populated, suggesting a low abundance of "superprimed" vesicles (Lee et al., 2013; Taschenberger et al., 2016) at hippocampal mossy fiber synapses in our experimental conditions.

Figure S5, related to Figure 3. Dependence of PTP on extracellular Ca^{2+} concentration

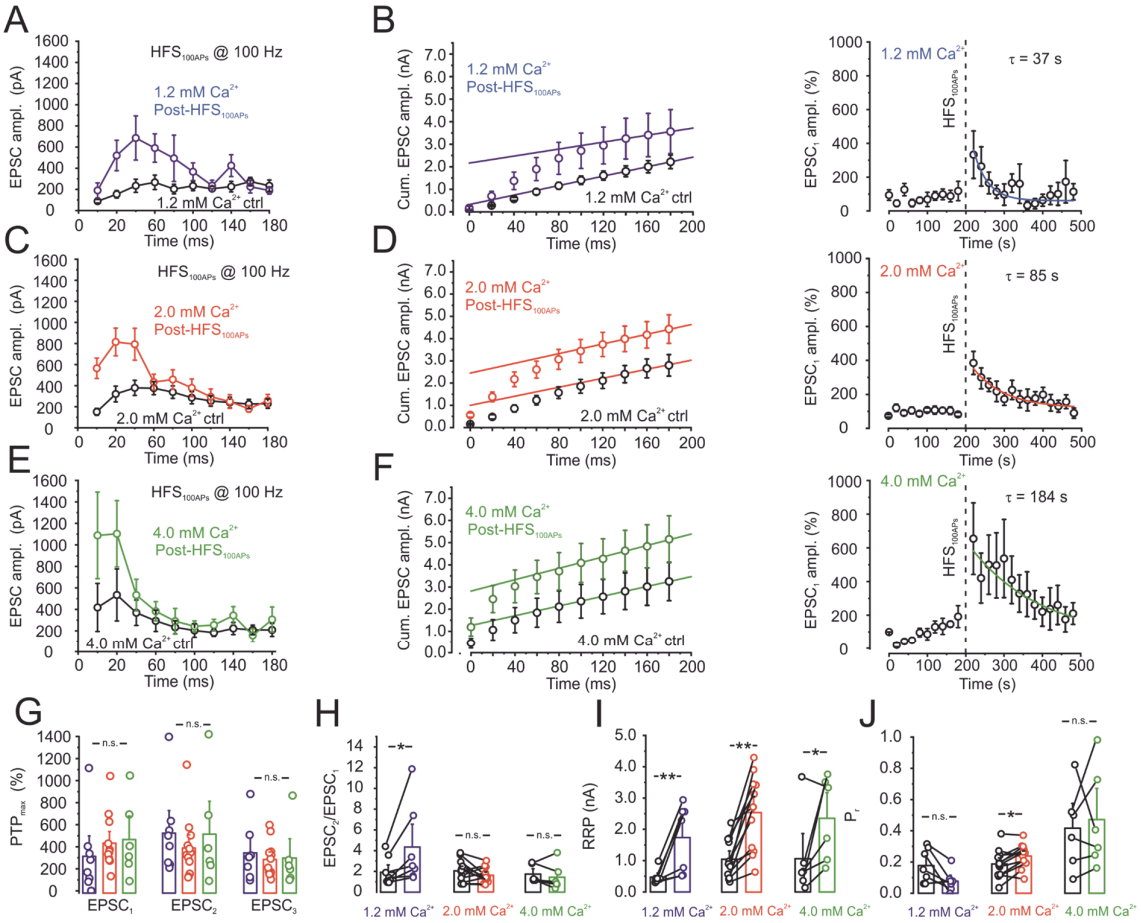

(**A** and **B**) Plot of EPSC amplitude during 50-Hz test trains of 10 stimuli under control conditions (black) and after HFS_{100APs} (purple) in 1.2 mM extracellular Ca^{2+} (A), plot of cumulative EPSC peak amplitude (B, left), and plot of average EPSC peak amplitude against experimental time for first EPSC (B, right). HFS_{100APs} was applied at the time point indicated by the vertical dashed line. Curve in (B, right) indicates exponential function fit to the PTP decay phase.

(**C–F**) Similar plot as in (A and B), but for 2 mM Ca^{2+} (C and D) and 4 mM Ca^{2+} (E and F).

(**G**) Summary bar graph of PTP for 1.2, 2, and 4 mM extracellular Ca^{2+}.

(**H**) Summary of paired-pulse ratio ($EPSC_2$ / $EPSC_1$) in 1.2, 2, and 4 mM Ca^{2+}. Note that paired-pulse ratio paradoxically increases after PTP induction in 1.2 mM Ca^{2+}.

(**I** and **J**) Summary bar graph of changes in RRP (I) and P_r (J) after PTP.

In total, data were obtained from 9 mossy fiber terminal–CA3 pyramidal neuron recordings. *, $p < 0.05$; **, $p < 0.01$.

Figure S6, related to Figure 5. Functional EM reveals pool overfilling after PTP induction

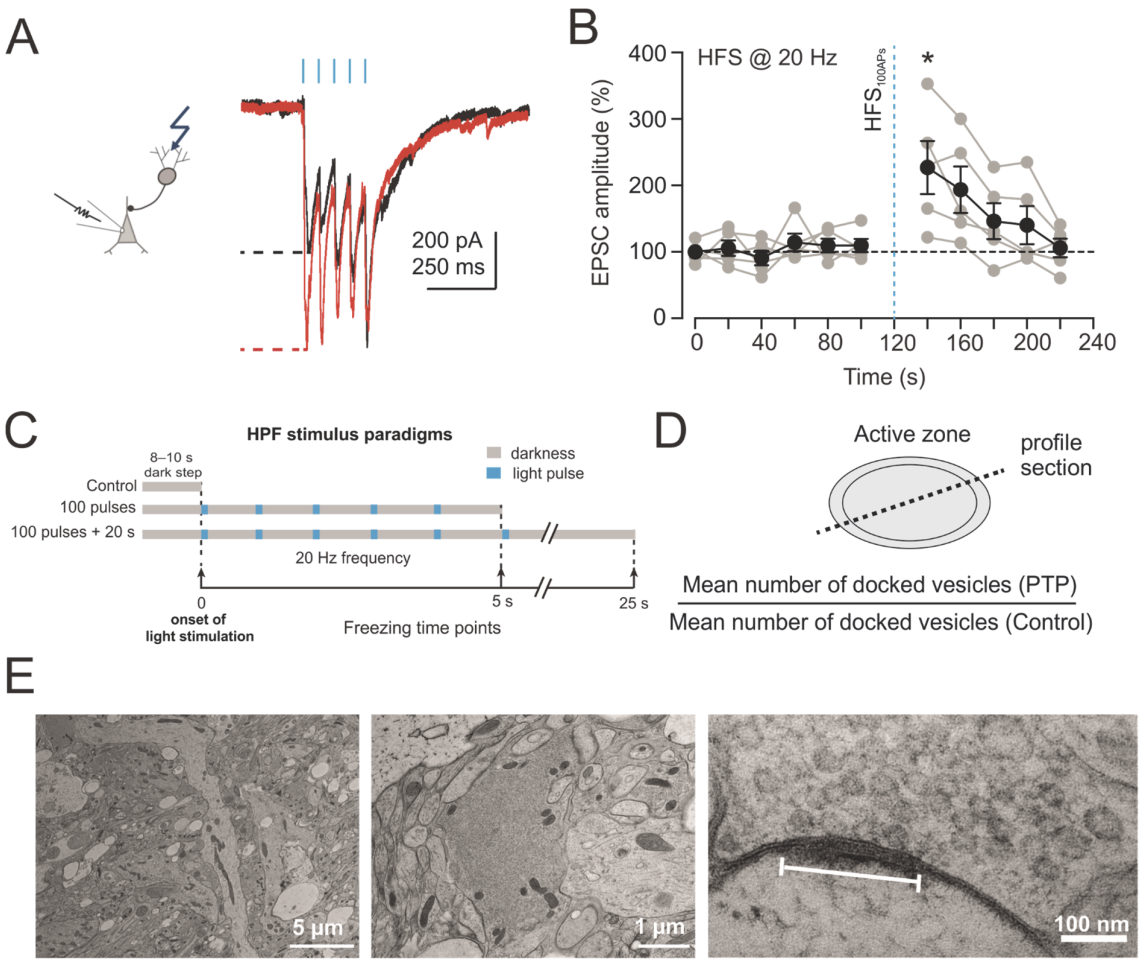

(**A**) Optogenetically evoked EPSCs in CA3 pyramidal neurons. Black, control; red, trace after HFS_{100APs}. Blue lines indicate light pulses.
(**B**) Plot of EPSC peak amplitude against time before and after HFS_{100APs}. Gray, individual experiments; black, average from 5 recordings. Blue vertical dashed line indicates HFS_{100APs}. Recordings were performed at near-physiological temperature (Borges-Merjane et al., 2020). *, $p < 0.05$.
(**C**) Schematic illustration of stimulation–freezing paradigms used in the present set of experiments.
(**D**) Schematic illustration of analysis of number of docked vesicles per profile. Note that the number of vesicles per active zone (a 2-dimensional structure) is expected to be quadratically related to the number of vesicles per profile (a 1-dimensional structure).
(**E**) Electron micrographs of hippocampal mossy fiber synapses at different magnification. White bar in right micrograph indicates postsynaptic density.

Figure S7, related to Figure 7 and Discussion. Unique mechanisms of PTP enable flexible synaptic computations.

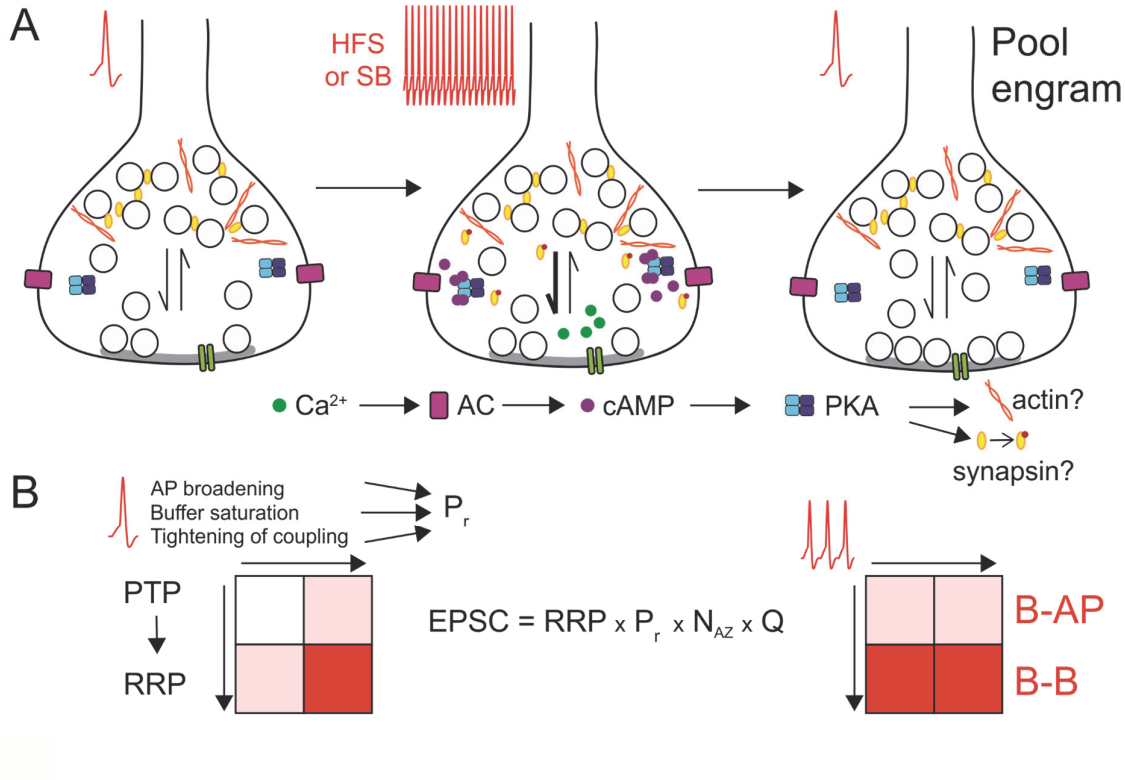

(**A**) Mechanisms of PTP induction. Sensitivity of PTP to PKA blockers and actin polymerization inhibitors suggest that HFS enhances refilling of readily releasable and docked vesicle pools. A possible molecular link between PKA and actin is represented by synapsin (Gitler et al., 2008).

(**B**) Orthogonal forms of presynaptic plasticity at hippocampal mossy fiber synapses enable flexible synaptic computations. Left, AP broadening, buffer saturation, and tightening in source-sensor coupling are known to change release probability during facilitation or long-term potentiation (Geiger and Jonas, 2000; Vyleta and Jonas, 2014; Midorikawa and Sakaba, 2017). In contrast, PTP primarily increases pool size. As the EPSC peak amplitude is the product of RRP, release probability (P_r), number of active zones (N_{AZ}), and quantal size (Q), changes in RRP and P_r may affect synaptic efficacy multiplicatively (as indicated by color intensity). Right, changes in RRP and P_r could differentially regulate mossy fiber detonation (Henze et al., 2002; Vyleta et al., 2016). Increase in RRP promotes a burst-to-burst transmission mode, whereas increase in P_r shifts the synapse towards a burst-to-spike transmission regime.

Table S1, related to Figure 2. Basic properties of unitary EPSCs at hippocampal mossy fiber–CA3 pyramidal neuron synapses

Parameter	**Value before PTP (mean ± SEM, n pairs)**	**Value after PTP (20 s)**
Synaptic delay (ms)	1.47 ± 0.08 (n = 12)	1.45 ± 0.15 (n = 12)
20–80% EPSC rise time (ms)	0.9 ± 0.07 (n = 12)	1.1 ± 0.09 (n =12)
EPSC peak amplitude (pA)	180.8 ± 55.16 (n = 12)	564.5 ± 97.05 (n = 12)
EPSC decay time constant (ms)	6.9 ± 0.42 (n = 12)	5.6 ± 0.28 (n = 12)
PTP (%) Induction by HFS_{100APs}	432 ± 74 (n = 12)	
Mossy fiber mEPSC peak amplitude (median)	41.8 ± 3.3 (n = 8)	45.7 ± 3.6 (n = 8)
Mossy fiber mEPSC peak amplitude (mean)	52.9 ± 3.2 (n = 8)	59.9 ± 4.2 (n = 8)
Total mEPSC peak amplitude (median)	29.9 ± 1.5 (n = 13)	

Evoked EPSC experiments were performed with presynaptic tight-seal cell-attached stimulation.

Miniature EPSC (mEPSC) experiments were performed in the presynaptic whole-cell configuration. Mossy fiber mEPSCs were recorded during presynaptic depolarization. Total miniature mEPSCs (including both mossy fiber and non-mossy fiber contributions) were collected during the entire recording time.

Values indicate mean ± SEM. PTP was induced by HFS_{100APs}.

Table S2, related to Figure 3. Vesicle pool model describing EPSC train responses

Parameter	Optimal value
N	23.1
r_{01}	85.5 ms^{-1}
r_{10}	0.010 ms^{-1}
r_{12}	0.052 ms^{-1}
r_{21}	3.929 ms^{-1}
P_{r1}	0.173
P_{r2}	0.202
r_0	0.178 ms^{-1}
r_1	0.014 ms^{-1}
τ_r	918.3 ms
K_r	2.398
m_r	0.329
f_{max}	2.374
K_f	0.916
m_f	7.012
r_{spont}	2.824 10^{-6} ms^{-1}

Models were fit to all 7 data sets (10 pulses at 50 Hz for control conditions, 100 pulses at 100 Hz for HFS_{100APs}, and 5 times 10 pulses at 50 Hz for test conditions). Starting values were determined by a custom-made random search algorithm, and optimization was performed using a Brent's principal axis method. Parameter range was set to [0, 1000] for pool size N, [0–0.01, 100] for rates r, [0.0001, 1] for release probabilities P_r, [2, 1000] for facilitation factor f_{max}, [0.5, 100] for affinities K, [0.01, 10] for exponents m, and [0, 0.01] for spontaneous release rate r_{spont}. For details, see STAR Methods.